ORIGINAL ARTICLE

Reduction of complement factor H binding to CLL cells improves the induction of rituximab-mediated complement-dependent cytotoxicity

This article has been corrected since Advance Online Publication and an erratum is also printed in this issue

S Hörl[1,3], Z Bánki[1,3], G Huber[1], A Ejaz[1], D Windisch[1], B Muellauer[1], E Willenbacher[2], M Steurer[2] and H Stoiber[1]

A main effector mechanism of rituximab (RTX) is the induction of complement-dependent cytotoxicity (CDC). However, this effector function is limited, because CLL cells are protected from complement-induced damage by regulators of complement activation (RCAs). A prominent RCA in fluid phase is factor H (fH), which has not been investigated in this context yet. Here, we show that fH binds to CLL cells and that human recombinant fH-derived short-consensus repeat 18–20 (hSCR18–20) interferes with this binding. In complement-based lysis assays, CLL cells from therapy-naive patients were differently susceptible to RTX-induced CDC and were defined as CDC responder or CDC non-responder, respectively. In CDC responders, but notably also in non-responders, hSCR18–20 significantly boosted RTX-induced CDC. Killing of the cells was specific for CD20$^+$ cells, whereas CD20$^-$ cells were poorly affected. CDC resistance was independent of expression of the membrane-anchored RCAs CD55 and CD59, although blocking of these RCAs further boosted CDC. Thus, inhibition of fH binding by hSCR18–20 sensitizes CLL cells to CDC and may provide a novel strategy for improving RTX-containing immunochemotherapy of CLL patients.

INTRODUCTION

The monoclonal antibody (mAb) rituximab (RTX) was the first antibody approved by the US Food and Drug Administration for the treatment of cancer,[1] and has been successfully incorporated into therapeutic standards for aggressive and indolent non-Hodgkin's lymphomas.[2,3] Moreover, recent trials show that the addition of RTX to fludarabine-based chemotherapy improves complete response rates and prolongs progression-free survival, and, when given first-line, also improves overall survival.[4,5]

RTX is a genetically engineered chimeric murine-derived mAb (immunoglobulin G1) that recognizes CD20 on the surface of normal and malignant B cells.[6] Even though RTX has become a standard of care for a wide range of B-cell malignancies, the precise biological modes of action in humans have not been fully clarified.[2] Antibody-dependent cellular cytotoxicity (ADCC) and complement-dependent cytotoxicity (CDC) are considered to be the main antitumor effects of RTX.[7] Several studies propose antibody-dependent cellular cytotoxicity as the most critical effector mechanism of RTX in vivo.[8–10] In contrast, it was shown that the therapeutic activity of RTX was completely abolished in mice lacking C1q, whereas it was not affected in mice depleted of NK cells, neutrophils or T cells, demonstrating that complement activation is fundamental for RTX efficacy in vivo.[11] A study involving 21 CLL patients revealed that patients who failed to clear CLL cells from their blood after RTX therapy showed an increased expression of CD55 and CD59, indicating that, in

particular, complement-resistant cells evaded RTX treatment.[12] The complement system consists of multiple plasma proteins with effector function, soluble regulatory proteins and cell surface-anchored proteins with receptor or regulatory functions.[13] Activation of the complement system results in the destruction of cells by CDC.[14] To prevent the potentially harmful effect of complement activation on normal cells, several fluid-phase and membrane-bound regulators of complement activation (RCAs) have evolved to restrict activation at different levels of the complement cascade.[15] Similar to normal host cells, tumor cells express and bind RCAs to evade complement attack.[16] Thus, although therapeutic antibodies are strong triggers for complement activation and complement deposition on tumor cells has been demonstrated, the efficacy of complement-mediated mechanisms may be diminished.[16] With CD55 and CD59, two membrane-anchored RCAs (mRCAs) have been identified as having a role in the protection of non-Hodgkin's lymphoma cells or CLL cells against complement attack (CD55[17] and CD59 on tumor cells does not predict clinical outcome after RTX treatment in follicular non-Hodgkin's lymphoma[18]). CD55 (decay-accelerating factor) binds to C3b and C4b, thereby accelerating the decay of C3 and C5 convertases.[19] CD59 targets late steps of the complement cascade and inhibits the lytic ability of the membrane attack complex.[20] Besides these mRCAs, fluid-phase complement inhibitors, such as factor H (fH),[19] might also account for the resistance of CLL cells to antibody-induced CDC. There is evidence that various primary tumors (breast

cancer, prostate cancer, lung cancer) and tumor cell lines (H2 glioblastoma cells, small-cell lung cancer cells) evade CDC, either by expressing fH or by binding it to their cell surface (genetic variations[21] and disease associations[22–26]). Complement fH is a soluble, single polypeptide-chain glycoprotein regulator (155 kDa) of the complement system that is present in the plasma at a concentration of 0.235–0.81 mg/ml (genetic variations[21] and disease associations[27]). fH has several modes of action: it binds C3b competitively to factor B, thereby inhibiting formation of the alternative pathway C3 convertase; it accelerates the decay of C3 and C5 convertases; and it acts as a cofactor for the factor I (fI)-mediated proteolytic cleavage of active C3b into inactive C3b (iC3b).[28] fH is composed of 20 short-consensus repeat (SCR) domains.[29] Detailed structure–function studies revealed distinct functional regions in the fH molecule. The complement regulatory activity is located within the N-terminal SCRs 1–4,[30] whereas the C3b and glycosaminoglycan binding sites are located within SCR7 and the C-terminal SCRs 19–20.[29,31–34]

For this study, we generated human fH-derived recombinant SCR18–20 (hSCR18–20), representing a main binding domain of fH. Here, we show that by replacing fH from the surface of primary CLL cells with hSCR18–20, cells were sensitized to RTX-induced CDC. Furthermore, we determined the relative contribution of fH, CD55 and CD59 to the protection of malignant B cells against CDC. Taken together, our results indicate that fH is a main component of the resistance of CLL cells to CDC, and thus affects the efficacy of RTX in CLL therapy.

MATERIALS AND METHODS

Recombinant SCRs
Human complement fH-derived proteins hSCR16–17 and hSCR18–20 were produced recombinantly and characterized as described in the Supplementary Material and Materials and methods section.

Isolation of primary CLL cells
This study was approved by the Ethics Committee of Innsbruck Medical University. Patient characteristics are summarized in Supplementary Table 1. Heparinized peripheral blood from therapy-naive CLL patients was obtained at the Department of Hematology and Oncology, Innsbruck Medical University (Innsbruck, Austria), after receiving informed consent. Peripheral blood mononuclear cells (PBMCs) were separated on a Ficoll gradient (GE Healthcare, Vienna, Austria) and cultured overnight in RPMI 1640 medium (Gibco, LifeTech Austria, Vienna, Austria) supplemented with 10% fetal calf serum (Gibco) and glutamine (Gibco). Cells were stimulated with 0.5 μg/ml lipopolysaccharide (Sigma, St Louis, MO, USA). The B-cell fraction of PBMCs was on average 87% as determined by flow cytometry, measuring the frequency of CD20-expressing cells (data not shown).

Flow cytometry
Mouse anti-human CD55 (clone IA10) and mouse anti-human CD59 (clone p282) monoclonal Abs were purchased from BD Pharmingen (Heidelberg, Germany). PBMCs were incubated with Abs against human CD55 or human CD59 for 30 min at 4 °C. After washing, cells were stained with fluorescein isothiocyanate-conjugated polyclonal goat anti-mouse immunoglobulin G. In addition, detection of CD20 expression was performed by incubating cells with RTX for 30 min at 4 °C. After washing, cells were stained with fluorescein isothiocyanate-conjugated rabbit anti-human immunoglobulin G. Samples were analyzed on a FACS Canto II cytometer (Becton Dickinson, Franklin Lakes, NJ, USA).

CDC assay
PBMCs (2×10^5 cells) were mixed with RTX at a concentration ranging from 1 to 100 μg/ml in the absence or presence of hSCR18–20 (1200 μg/ml), hSCR16–17 (1200 μg/ml), monoclonal mouse anti-human CD55 (blocking: clone HD1A; non-blocking: clone 1A10) or CD59 (blocking: clone MEM43; non-blocking: clone P282; all 10 μg/ml). Neutralizing antibodies HD1A and MEM43 were a generous gift from Dr C Harris (Cardiff University School of Medicine, Cardiff, UK). According to the experimental design, antibodies and recombinant proteins were applied either alone or in different combinations. Pooled normal human serum (NHS; derived from six healthy individuals) or heat-inactivated normal human serum (hiNHS) was added in a 1:4 dilution. Samples were incubated for 1 h at 37 °C. Following incubation, propidium iodide (PI) staining was performed to exclude dead cells. Finally, PI-negative viable cells were measured by counting these cells for 60 s at a constant flow rate on a FACS Canto II cytometer. One hundred percent survival was defined by counting viable cells in samples from CLL patients containing hiNHS only. The survival rates were calculated according to the formula: percent survival = 100% survival × count of viable cells in treated sample/count of viable cells in hiNHS control sample. CDC assay was also performed with the fibroblast cell line BHK-21 and epithelial cell line Colo-699.

To further investigate the selectivity of lysis, PBMCs from a CLL patient and PBMCs from a healthy donor were mixed to obtain a heterogeneous cell suspension with balanced T- and B-cell populations. The $CD3^+$ T-cell and $CD19^+$ B-cell fractions were identified by flow cytometry. The mixture was incubated with RTX in the absence or presence of hSCR18–20 (1200 μg/ml) under standard conditions (25% NHS or hiNHS, 1 h at 37 °C). Before flow cytometric analysis, cells were stained with allophycocyanin-Cy7-conjugated anti-human CD3 (clone HIT3a) (BioLegend, Vienna, Austria) and allophycocyanin-conjugated anti-human CD19 (clone HIB19) (BioLegend). PI-negative viable cells were counted in the $CD3^+$ T-cell and the $CD19^+$ B-cell gates, respectively. The survival rates for both populations were calculated with reference to the hiNHS control. Alternatively, mixed CDC assay was performed with CLL cells and polymorphonuclear neutrophilic (PMN) leukocytes isolated from pellets of Ficoll centrifugation derived from peripheral blood of healthy donors. Erythrocytes were removed by hypotonic lysis. Purified PMN suspensions contained >90% of $CD11b^+$ PMNs as determined by flow cytometry.

Western blot analysis for the detection of fH or C3 fragments
Western blot analysis was performed to investigate the binding of fH to CLL cells. For this, cells (2×10^5) were incubated with NHS as a source of fH (25% final concentration) in the absence or presence of hSCR18–20 (1200 μg/ml). Following incubation, cells were washed two times with phosphate-buffered saline and the pellet was lysed. Cell lysates were analyzed on an 8% gel under reducing conditions. Following transfer, the blot was developed with a polyclonal goat anti-human fH (Quidel, San Diego, CA, USA) as first and a horse radish peroxidase-conjugated mouse anti-goat immunoglobulin G as a second Ab. Signals were visualized by ECL according to the manufacturer's instructions. To analyze the binding of hSCR18–20 to CLL cells and its effect on fH, CLL cells were incubated with different concentrations of hSCR18–20 in the presence or absence of human recombinant fH (10 μg/ml; Quidel). Western blot analysis was performed as described above.

To determine whether hSCR18–20 affects the fH-mediated processing of C3b fragments, CLL cells were incubated with RTX alone (20 μg/ml) or RTX combined with hSCR18–20 (1200 μg/ml). NHS (25%) was added as a source of complement. Control samples were performed by incubating cells with hSCR only or together with 25% hiNHS or NHS in the absence of RTX. The reaction was stopped after the indicated periods of time by adding 50 mM EDTA. Cells were washed two times and western blot was performed as described above, except that as a first Ab goat anti-human C3 Ab (Complement Technology Inc., Tyler, TX, USA) was used to detect the C3 fragments.

Statistical analysis
Statistical analysis was performed using the GraphPad Prism software (La Jolla, CA, USA). The difference between CD20, CD55 and CD59 expression levels and effects of hSCR18–20 in comparison with RTX alone were determined by unpaired t-test. The dependence of CD20 expression levels and lysis rates was analyzed by means of Pearson's correlation. One-way analysis of variance was performed to evaluate the impact of hSCR18–20 and/or blocking antibodies alone and synergistically. To analyze the effect of blocking antibodies and hSCR18–20 as compared with their controls, a t-test for unpaired data was performed.

RESULTS

Displacement of fH by hSCR18–20 prolongs the presence of active C3b α′-chain on the surface of CLL cells
To visualize the binding of fH by western blot analysis, CLL cells were incubated with NHS (1:4 dilution) as a source of fH in the
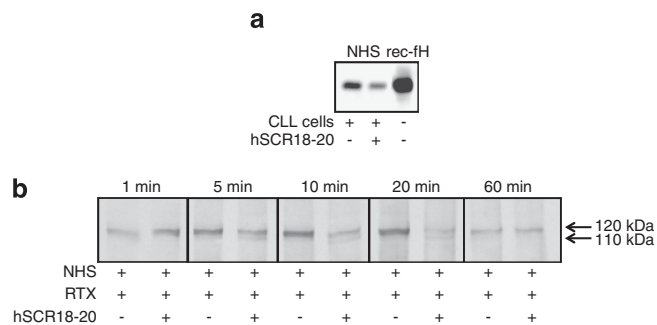
a

b

Figure 1. Displacement of fH from the surface of CLL cells by hSCR18–20 prolonged the presence of active C3b fragments. (**a**) To investigate the impairment of fH binding by hSCR18–20, CLL cells were incubated with NHS as a source of fH (lanes 1 and 2) in the presence or absence of hSCR18–20, as indicated. As control, recombinant fH was loaded on the gel in the absence of CLL cells (lane 3). hSCR18–20 clearly reduced the amount of fH binding to CLL cells. One of three independent experiments is shown. (**b**) Processing C3 fragments on the surface of CLL cells in the presence or absence of hSCR18–20 was investigated by incubating the cells with NHS in the presence of RTX with or without hSCR18–20 for different time points. Western blot analysis revealed that after 5 min of incubation, the 110 kDa α'-chain of active C3b appeared in the presence of hSCR18–20 and was visible at least for 20 min of incubation (lower panel). In contrast, nearly no active C3b fragments were detectable in the absence of hSCR18–20 in RTX alone.

absence or presence of hSCR18–20, as indicated in Figure 1a. To avoid CDC, no RTX was added. A distinct signal at 150 kDa was obtained from serum-derived fH (lane 1) that bound to CLL cells. As control, purified recombinant fH was applied to the gel (lane 3). In the presence of hSCR18–20, the fH signal was clearly reduced (Figure 1a, lane 2), indicating that the SCR interferes with the binding of fH to the cell surface. Owing to its cofactor activity, displacement of fH by hSCR18–20 might impair the fI-mediated inactivation of C3b on the cell surface. Thus, CLL cells were incubated with NHS in the presence of RTX with or without hSCR18–20 at different time points. As control hiNHS was used. After washing, western blot analysis was performed to detect C3-cleavage products deposited on the cell surface. After 1 min of incubation both 120 kDa α-chain and 75 kDa β-chain of C3 were clearly detected in all samples (Supplementary Figure 2). After 5 min, both α$_1$-chain of iC3b (68 kDa) and C3dg/C3d were detectable in the presence of both RTX and RTX/SCR18–20 owing to the processing of C3 upon complement activation induced by RTX (Supplementary Figure 2). After 5 min of incubation, 110 kDa α'-chain of active C3b appeared in the presence of hSCR18–20 and was visible at least for 20 min of incubation (Figure 1b). In contrast, hardly any active C3b were detectable in the absence of hSCR18–20 and the presence of RTX, suggesting a rapid inactivation of C3b to iC3b (Figure 1b).

Further analyzing the displacement of fH by hSCR18–20 revealed a concentration-dependent binding of hSCR18–20 to CLL cells (Figure 2a), which resulted in a dose-dependent reduction of fH binding when fH (Figure 2b).

Recombinant hSCR18–20 enhances RTX-mediated CDC on primary CLL cells

Next, we analyzed whether the reduction in fH binding sensitizes CLL cells and enhances CDC. For this, we performed CDC assays with freshly isolated PBMCs from 37 CLL patients. The B-cell fractions from patient samples were determined by flow cytometric analysis and ranged from 76 to 98%, with a mean of 87% (data not shown). CLL cells were incubated with increasing concentrations of RTX (1–100 μg/ml) in the absence or presence of hSCR18–20 under standard conditions (25% NHS, 1 h, 37 °C).
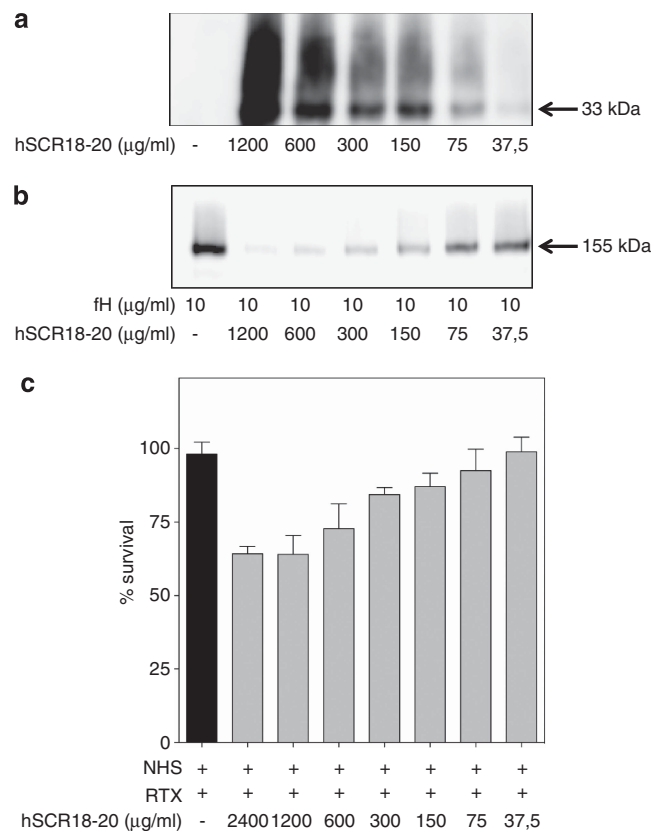
a

b

c

Figure 2. Concentration-dependent binding of hSCR18–20 to CLL cells displaced fH and subsequently resulted in a concentration-dependent enhancement of CDC. (**a**) Concentration-dependent binding of hSCR18–20 to CLL cells. CLL cells were incubated with different concentrations of hSCR18–20, and after washing lysate of the cell, the pellet was analyzed by western blot using polyclonal Ab against human fH. Figure shows one representative of three independent experiments. (**b**) Concentration-dependent displacement of fH by hSCR18–20. CLL cells were incubated with different concentrations of hSCR18–20 in the presence of human recombinant fH. Following incubation, cells were washed two times with phosphate-buffered saline, the pellet was lysed and the western blot was performed using polyclonal Ab against human fH. The figure shows one representative of three independent experiments. (**c**) Concentration-dependent enhancement of CDC in the presence of hSCR18–20. CLL cells were incubated with NHS and RTX in the presence or absence of different hSCR18–20 concentrations. PI-negative viable cells were determined by fluoresence-activated cell sorter. One hundred percent survival was defined by counting viable cells in samples from CLL patients containing hiNHS only. Data represent mean of three independent experiments. Error bars: s.e.m.

We used 1200 μg/ml of hSCR18–20 in our experiments, as this concentration reached the highest efficacy in CDC assay (Figure 2c). Survival rates for CLL cells were measured after the addition of PI by flow cytometric analysis counting the PI-negative viable cells. First, we investigated the CDC of primary CLL cells induced by RTX. In line with previous observations,[18,35] we detected a concentration-dependent, varying sensitivity to RTX-induced CDC among the patient samples. At the maximum RTX concentration of 100 μg/ml, 29 out of 37 (78%) patients showed no or very poor RTX-induced CDC and were considered CDC non-responders (cutoff value of <25% lysis; Figure 3a, open circles). Out of 37 samples, 8 (22%) CDC responders were identified, who showed lysis ranging between 27 and 66% at the highest antibody concentration (Figure 3b, open circles). Most importantly, addition of hSCR18–20 (1200 μg/ml) enhanced RTX-induced CDC in both
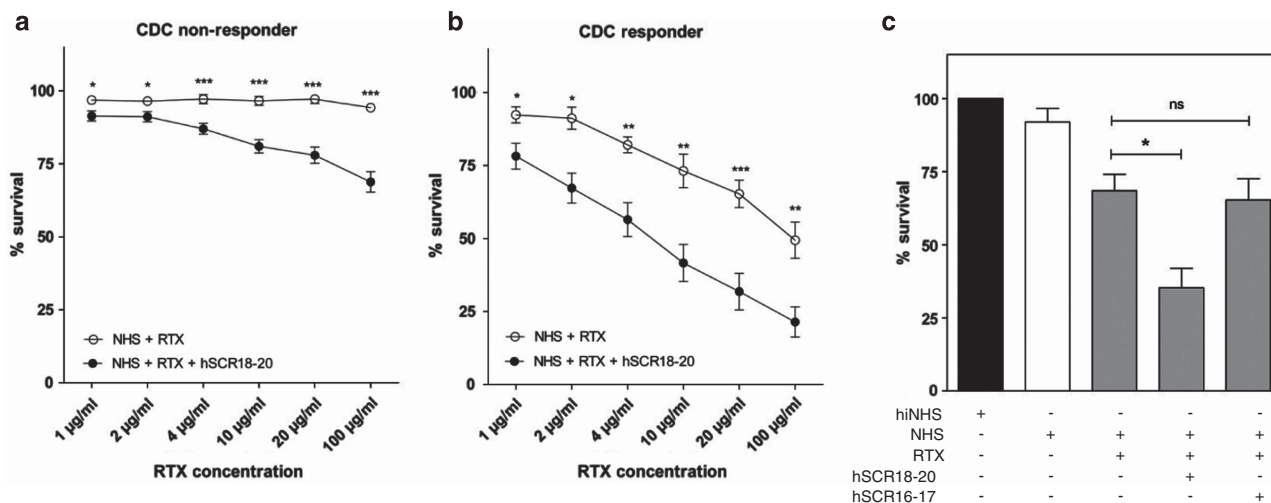
Figure 3. fH-derived SCR18–20 reduced binding of fH to CLL cells and enhanced RTX-induced CDC. (**a**) Out of 37 patient samples tested, 29 CLL preparations (i.e. 78%) displayed a CDC non-responder phenotype, which was defined by a cutoff value of <25% cell lysis (open circles) at the highest RTX concentration tested. Addition of hSCR18–20 improved CDC significantly (closed circles; *$P < 0.05$; **$P < 0.01$; ***$P < 0.001$) and turned non-responder into responder samples at the highest RTX concentrations tested in the assay. Circles: mean of 29 patients; bars: s.e.m. (**b**) In total, 8 of 37 patients were CDC responders with > 25% cell lysis (open circles). Similar to the non-responder group, the presence of hSCR18–20 improved CDC (closed circles) in responder samples, resulting in the clearance of >75% of CLL cells at the highest RTX concentration tested. Circles: mean of eight patients; bars: s.e.m. (**c**) CLL cells were treated in standard CDC assays with 20 µg/ml RTX in the absence or presence of hSCR18–20 or hSCR16–17, as indicated. The survival rate was 68.53% after treatment with RTX alone and was clearly reduced by the addition of hSCR18–20 (35.26), but not hSCR16–17 (65.33). The result (combined from three patients) was significant ($P = 0.0375$). Error bars: s.e.m. NS, nonsignificant.

CDC responders (Figure 3b, closed circles) and non-responders (Figure 3a, closed circles). This enhancement of RTX-mediated CDC by hSCR18–20 was significant at all RTX concentrations. Enhancement of RTX-mediated CDC of CLL cells by hSCR18–20 was most probably due to the reduced binding of fH to the cell surface, as hSCR16–17 representing fH-derived non-binding control domain did not influence RTX-induced CDC (Figure 3c). The assay was robust and highly reproducible; three independent experiments performed with samples from the same donor gave highly comparable results (Supplementary Figure 3).

Enhancement of RTX-mediated CDC by hSCR18–20 is specific to B cells

Next, we proved the specificity of RTX-induced CDC. For this, PBMCs from a healthy donor were mixed with PBMCs from a CDC responder patient, resulting in balanced CD3$^+$ T-cell and CD19$^+$ B-cell fractions in the mixture (Figure 4a, dot plot). The CDC assay was performed under standard conditions as described above, except that before PI staining, cells were costained with allophycocyanin-conjugated mouse anti-human CD19 and allophycocyanin-Cy7-conjugated mouse anti-human CD3 mAbs. PI-negative viable cells were then counted in CD3$^+$ T-cell and CD19$^+$ B-cell populations. Compared with samples incubated in NHS alone, the counts for PI-negative viable cells in the CD19$^+$ B-cell population were reduced in samples incubated with RTX. After treatment with RTX combined with hSCR18–20, CLL cells almost disappeared (Figure 4a). By contrast, the counts for PI-negative viable cells in the CD3$^+$ T-cell population remained unchanged in all samples (Figure 4a). A similar pattern was obtained with three further patient samples (Figure 4b). Although in CDC assays the survival of CD3$^+$ T cells was not influenced by RTX and hSCR18–20 (Figure 4b, gray bars), we measured a decrease in survival of the CD19$^+$ B cells in the presence of RTX, which were significantly reduced when RTX was combined with hSCR18–20 (Figure 4b, black bars). Similar experiments were performed with isolated CD11b$^+$ PMNs mixed with PBMCs from a CLL patient. Following the CDC assay, cells were costained with

CD19 and CD11b mAbs before PI staining. PI-negative viable cells were then counted in CD11b$^+$ PMN and CD19$^+$ B-cell populations. Again, only marginal effects on the survival of PMNs in the presence of hSCR18–20 were found (Supplementary Figure 4a). Furthermore, neither erythrocytes (Supplementary Figure 4B), the fibroblast cell line BHK-21 (Supplementary Figure 4C) nor the epithelial cell line Colo-699 (Supplementary Figure 4D) showed significant CDC in the presence of hSCR18–20 and RTX.

Sensitivity of CLL cells to CDC correlated with CD20, but not with CD55 or CD59, expression on CLL cells

The amount of CD20 expressed on the cell surface was previously described to determine the CDC efficacy of RTX in various B-cell malignancies.[1,18,35,36] Thus, we analyzed the CD20 expression levels on CLL cells from all patients by flow cytometry. CD20 expression represented by the mean fluorescence intensity (MFI) was highly variable on CLL cells from the 37 patients and ranged from 3412 to 38 143 (Figure 5a). As compared with the CDC non-responder group, the expression of CD20 on CLL cells was significantly higher in CDC responder patients (Figure 5b). We found that at a concentration of 20 µg/ml RTX, CD20 expression on CLL cells correlated negatively with cell survival in CDC assays in the presence of RTX (Figure 5c). Moreover, CD20 expression on CLL cells showed a significant negative correlation with survival in CDC assays in the presence of RTX in combination with hSCR18–20 (Figure 5d).

mRCAs have been controversially discussed to affect the CDC efficacy of RTX (CD55)[17] and CD59 on tumor cells does not predict clinical outcome after RTX treatment in follicular non-Hodgkin's lymphoma[18,37]). Therefore, we also analyzed the expression of CD55 and CD59 on CLL cells in the CDC responder as well as in the non-responder group. MFI and thus expression levels of CD55 and CD59 varied on CLL cells among the 37 patients (Supplementary Figure 5A). In contrast to CD20, no significant difference in the expression of CD55 (Supplementary Figure 5B) or CD59 (Supplementary Figure 5C) on CLL cells between the CDC responder and the non-responder group was observed.
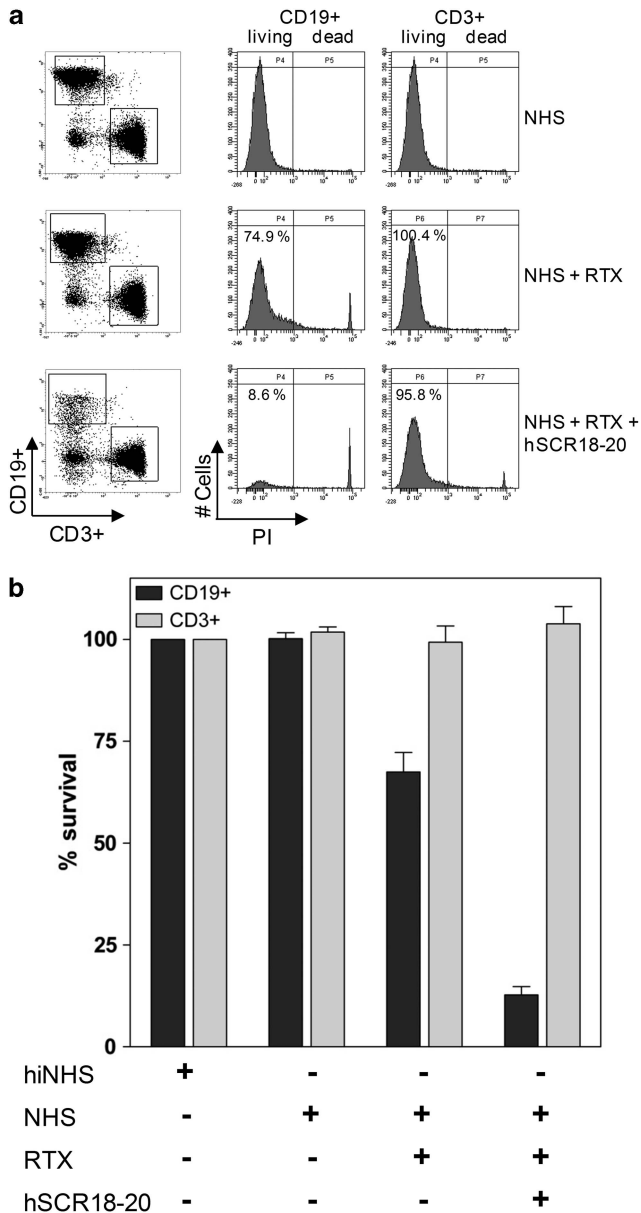
Figure 4. Lysis induced by RTX and hSCR18–20 was restricted to B cells. A mixture of CLL PBMCs and PBMCs from healthy donors was treated in the presence of NHS with RTX or RTX and hSCR18–20 in CDC assays. After staining, CD3$^+$ and CD19$^+$ cell populations were analyzed by fluoresence-activated cell sorter. (**a**) A decrease in the amount of PI-negative viable (x axis) was observed after treatment with RTX in the CD19$^+$ B-cell population. The combination of RTX and hSCR18–20 further reduced the viable B-cell population. In contrast, no shift was seen in the CD3$^+$ T-cell population. Results show a representative patient sample. (**b**) Treatment with RTX or RTX combined with hSCR18–20 reduced survival rates for CD19$^+$ B cells and killed 33% or 89% of the cells, respectively (dark gray bars). By contrast, CD3$^+$ T cells were not affected (99% and 104%; light gray bars). Survival rates were calculated with reference to the hiNHS control, which defined 100% survival. Error bars: s.e.m, $n = 3$.

Concerted action of fH and mRCAs in the protection of primary CLL cells against RTX-mediated CDC

mRCAs have been previously described as important factors influencing CDC efficacy in various types of malignant B cells.[15,18,35,37,38] As fH has never been considered in this context, we next performed CDC assays in the presence of blocking anti-CD55 (HD1A), blocking anti-CD59 (MEM43) or hSCR18–20. Cell count of PI-negative viable CLL cells in the hiNHS sample was considered 100% survival. Survival rates for other samples were calculated according to this control. In the absence of RTX, treatment of cells with either hSCR18–20 or blocking antibodies did not influence survival in the CDC assay (Figure 6a, gray bars). Next, the enhancement of RTX-mediated CDC by HD1A, MEM43 or hSCR18–20 alone or in different combinations was investigated (Figure 6b). Whereas HD1A (anti-CD55) and hSCR18–20 significantly triggered RTX-mediated CDC of CLL cells, blocking of CD59 functions by MEM43 showed only a slight improvement in CDC. HD1A and hSCR18–20 showed a synergistic effect in the improvement of RTX-mediated CDC, as the combination of both resulted in a significantly increased effect as compared with that of HD1A or hSCR18–20 alone (Figure 6b). CDC assays using the isotype-matched but non-blocking CD55 (clone 1A10) and CD59 (clone P282) mAbs were performed to estimate the contribution of putative complement activation made by the Fc portion of the antibodies. As non-blocking CD55 and CD59 Abs did not improve RTX-mediated CDC of CLL cells (Figures 6c and d), the enhancement of CDC by the corresponding blocking Abs is related to their capacity to abrogate CD55 and CD59 regulatory functions, rather than to additional induction of complement activation by the Fc portion of the antibodies.

DISCUSSION

The crucial role of fH in the protection of malignant cells was shown for several tumor cell types, but has never been considered in the context of malignant B cells. For this reason, we investigated the impact of fH in the resistance of primary CLL cells to RTX-induced CDC. As shown by western blot analysis, fH binds to CLL cells. Binding was impaired in the presence of fH-derived hSCR18–20, indicating that the C terminus of fH is involved in this interaction. This was not surprising, because it is known that the C-terminal region of fH binds to polyanionic surface proteins such as glycosaminoglycans, which are often overexpressed on tumor cells.[21–26] Whether different expression patterns of these negatively charged surface structures on CLL cells account for the observed responder or non-responder phenotype remain to be determined.

Here, we demonstrate that hSCR18–20 was able to break resistance and enhanced responsiveness to RTX-treated CLL cells from all patients tested. In addition, SCRs turned CDC non-responder into CDC responder phenotypes, and thus significantly improved the efficacy of RTX-mediated tumor cell lysis. Addition of hSCR18–20 to NHS and CLL cells in the absence of RTX had no effect on CDC induction. Thus, the biological response was not only dependent on the presence but also on the activation of complement. This is in line with our observation that CDC was specific for CLL cells. As RTX binds only to a minor population of T cells, which express CD20,[39] predominantly the B-cell fraction was lysed in the presence of RTX and hSCR18–20. In line, other cell types, that is, cells such as PMNs, erythrocytes, BHK-21 fibroblasts or Colo-699 epithelial cells, were not affected by the treatment with RTX and hSCR18–20.

Also, no direct RTX cytotoxicity was observed as indicated by cell resistance when hiNHS was used. This further indicates that active complement was the driving force for the clearance of the CLL cells in our experimental settings. Nevertheless, complement activation is tightly controlled by a rapid cleavage, and thus inactivation of C3b generated during complement activation, referred to as iC3b. The displacement of fH from the cell surface might affect this processing of C3. In its absence, the cofactor activity of fH for the fI-mediated cleavage of active C3b (α′-chain) into iC3b and C3d might be affected. Besides, impaired fH binding may reduce the decay of the convertases, which would also promote the formation of the lytic pathway and CDC induction. Thus, the mechanism behind the enhanced CDC by hSCR18–20
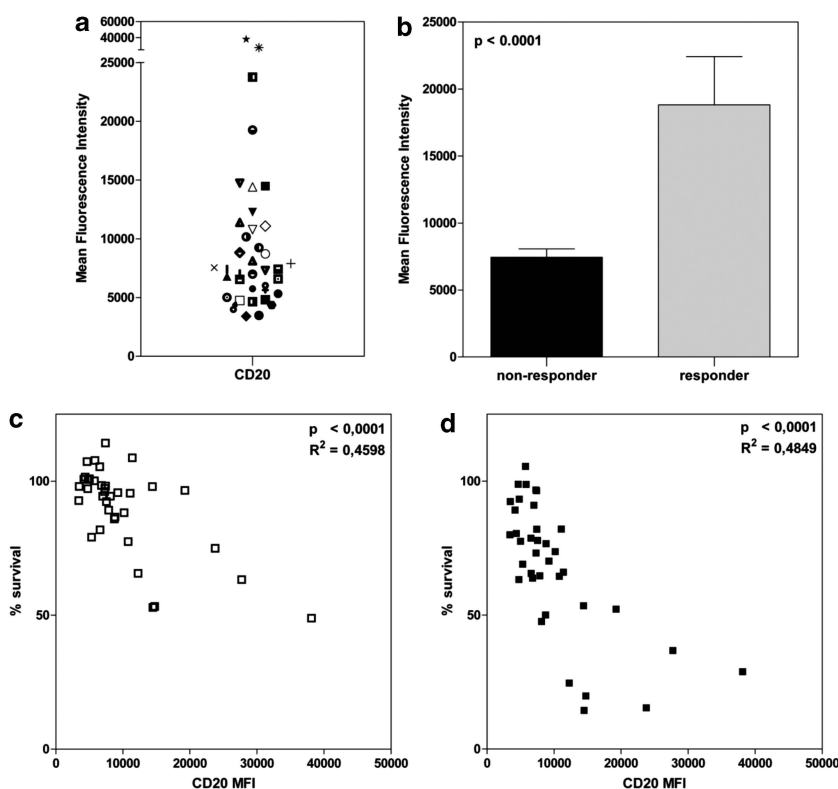
Figure 5. CD20 expression level determined the susceptibility of primary CLL cells to CDC. (**a**) The MFI of CD20 was determined by flow cytometric analysis in all patient samples. The MFI of CD20 varied highly among the 37 patient samples, namely from 3412 to 38 143. (**b**) CD20 expression levels were significantly higher ($P < 0.0001$) in CDC responder patients (gray bar) than in CDC non-responder patients (black bar). The statistical analysis was performed by t-test for unpaired data. Bars: s.e.m. (**c**) Plotting the MFI of CD20 against the lysis induced by $20\,\mu g/ml$ RTX showed a highly significant correlation ($P < 0.0001$). (**d**) Similarly, when the MFI of CD20 was plotted against the lysis induced by $20\,\mu g/ml$ RTX combined with hSCR18–20, a significant correlation was obtained ($P < 0.0001$).

might be a prolonged stability of the active form of C3b. Indeed, active C3b, represented by the 110 kDa α'-chain in western blot analysis, was visible even after an incubation period of 20 min when hSCR18–20 was present. By contrast, in the absence of hSCR18–20, active α'-chain disappeared after 10 min, most likely indicating a rapid inactivation of C3b.

Although the complement is indispensable for the RTX-induced clearance of tumor cells in various mouse models,[10,40] the precise mode of action of RTX in humans is still not clear.[41] Besides CDC, antibody-dependent cellular cytotoxicity and CR3-dependent phagocytosis may have important roles in clearing CLL cells in RTX-treated patients,[41] which displayed a CDC-resistant phenotype and exhibited $<25\%$ cell lysis. A similar refractory phenotype was also described by others, showing that only 6 out of 22 patient samples treated with RTX and complement had more than 10% cytotoxicity.[42] In contrast, therapeutic administration of fresh-frozen plasma as a source of complement enhanced the efficacy of RTX in CLL patients[43] with a treatment response of 72.7%.[44] Whether this clearance of CLL cells is due to enhanced lysis or CR3- or FcgR-dependent phagocytosis of tumor cells remains to be determined.

Susceptibility of RTX-treated CLL cells *in vitro* correlated with the expression levels of CD20, as has been shown by other groups.[36] In contrast to CD20, the expression levels of CD55 and CD59 had no impact on the susceptibility for CDC. Nevertheless, blocking of CD55 and CD59 identified these mRCAs as further regulators of CDC. This is in line with several publications showing that both CD55 and CD59 contribute to the resistance of various B-cell lymphomas such as CLL or follicular non-Hodgkin's lymphoma.[17,36,37] The minor contribution of CD59 observed in our experiments may be because of the use of various B-cell lines

by other investigators, which may differ in their biological response from isolated primary patient material used in this study. In addition, the use of different Ab clones, which bind with various affinities to CD59, may contribute to apparent discrepancies between our study and published results. This may also explain conflicting observations by Qin's group, which showed enhanced CDC on RTX-sensitive RL-7 lymphoma cells and RTX-induced resistant RR51.2 cells[15] with ILYD4, a bacterially derived inhibitor of CD59.[45] Our data indicate that mRCAs and fH, a fluid-phase RCA, contribute to the protection of CLL cells against CDC. Although not directly comparable, as the mAb against CD55 and a peptide (i.e. hSCR18-20) bind with different affinities to cells, blocking of either CD55 or fH induced similar toxicity for the tumor cells. CDC was boosted by the simultaneous inhibition of both RCAs, implying a synergistic mode of action. The central role of fH as negative regulator of complement is further underscored by recent findings showing that a single-nucleotide polymorphism in the fH gene locus (rs1065489) is associated with event-free survival in patients with follicular lymphoma and B-cell lymphoma in patients under RTX therapy.[46] These results indicate that interindividual differences in fH binding may increase RTX-mediated complement activation and thus enhance susceptibility to CDC in a manner similar to that recently discussed for meningococcal infections.[47] Although we excluded a contribution of fH polymorphisms and concentrations by using the same serum pool of healthy donors in all our CDC assays, we cannot rule out that fH variability mentioned above may account for differences to RTX responses between individual patients *in vivo*.

Thus, besides the known mRCA CD55 and also CD59, the fluid-phase RCA fH has to be considered as an additional factor that
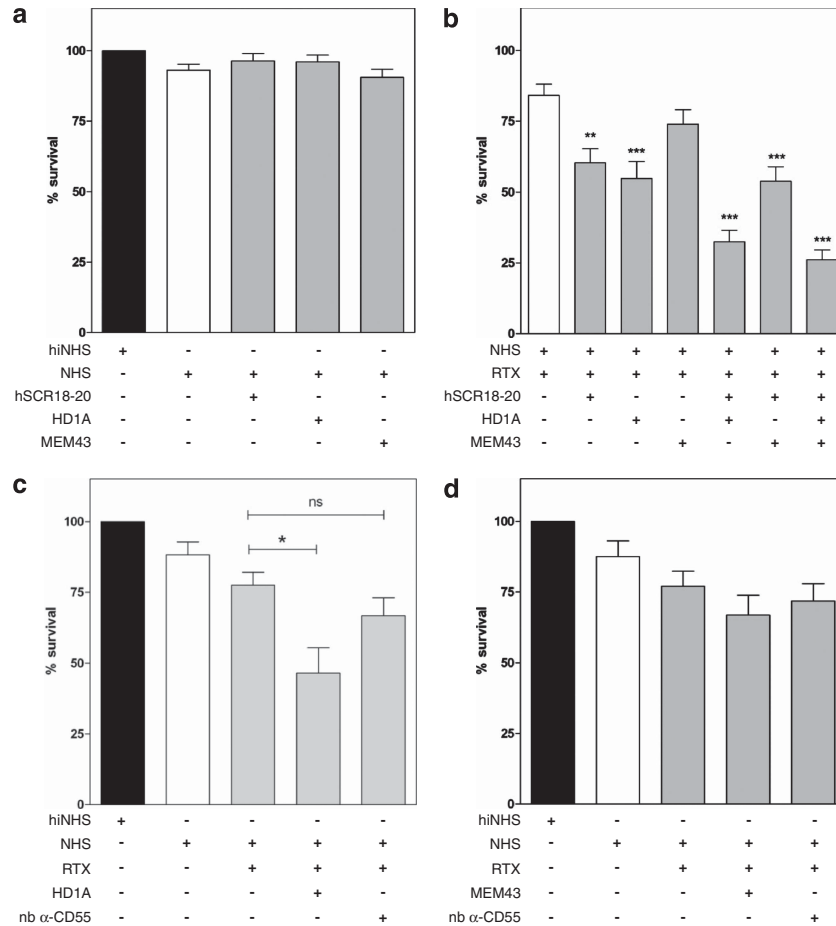
Figure 6. Effects of hSCR18–20, HD1A and MEM43 on RTX-induced CDC of primary CLL cells administered alone or in combination. (**a**) Patient cells were treated with RTX in the absence or presence of blocking anti-CD55 (HD1A), blocking anti-CD59 (MEM43) or hSCR18–20 under standard conditions. Addition of HD1A and hSCR18–20 significantly enhanced RTX-induced CDC (29% and 24%, respectively), whereas the blocking of CD59 by MEM43 showed minor improvement (10%). Combination of HD1A and hSCR18–20 resulted in significantly enhanced effects as compared with the effects of each compound individually. Survival rates were calculated according to the hiNHS control, which defined 100% survival. Error bars: s.e.m, $n = 20$. (**b**) Treatment of primary CLL cells with HD1A, MEM43 or hSCR18–20 and active complement in the absence of RTX did not induce CDC (gray bars), as compared with the NHS control (white bar, $n = 16$). (**c**) Improvement of RTX-induced CDC by blocking anti-CD55 (HD1A) was significant ($P = 0.0019$) in comparison to non-blocking anti-CD55 ($n = 7$). (**d**) No significant difference between the blocking anti-CD59 (MEM43) and non-blocking anti-CD59 was observed ($n = 6$). Survival rates were calculated according to the hiNHS control, which defined 100% survival. Error bars: s.e.m.

affects the biologic response of B lymphoma cells to the efficacy of RTX *in vitro* and likely also *in vivo*. Owing to the high concentrations necessary to impair fH binding, the direct application of SCR18–20 is not feasible *in vivo*. With serum concentration of fH ranges from 0.235 to 0.81 mg/ml, a direct inhibition of fH by mAbs may also be hampered by high amounts of Ab needed to be effective. Thus, SCR18–20 has to be coupled directly to RTX, which may provide several advantages: (i) the low-affinity peptide would be shuttled by RTX specifically to CD20-expressing cells and compete with fH directly on the spot; (ii) when directed with high affinity of the therapeutic Ab preferentially to CLL cells, lower amounts of SCR might be needed; (iii) improved serum stability; (iv) owing to the increased efficacy, such a bifunctional RTX-SCR molecule may turn patients susceptible to the Ab therapy, which are refractory to RTX treatment. The feasibility of such a strategy has only recently been demonstrated by our group showing an improved complement-mediated virolysis when SCR18–20 was linked to a virus-specific Ab (Huber *et al*, submitted).

In summary, we have shown that in addition to CD55 and CD59, binding of fH is a relevant mechanism for the resistance of CLL

cells to RTX-induced CDC. Inhibition of fH by means of recombinant fH-derived SCR18–20 molecules may be able to further ameliorate RTX-containing therapies in CLL, similar to other alternative approache,[48,49] and thus merits further investigation.

CONFLICT OF INTEREST

The authors declare no conflict of interest.

AUTHOR CONTRIBUTIONS

SH, ZB, BM performed experiments; GH, AE, DW, EW provided reagents, material and analysis tools; SH, ZB, MS, HS analyzed the data; and SH, ZB, MS, HS wrote the manuscript.

REFERENCES

1 Zhou X, Hu W, Qin X. The role of complement in the mechanism of action of rituximab for B-cell lymphoma: implications for therapy. *Oncologist* 2008; **13**: 954–966.

2 Cartron G, Trappe RU, Solal-Céligny P, Hallek M. Interindividual variability of response to rituximab: from biological origins to individualized therapies. *Clin Cancer Res* 2011; **17**: 19–30.

3 Foon KA, Hallek MJ. Changing paradigms in the treatment of chronic lymphocytic leukemia. *Leukemia* 2010; **24**: 500–511.

4 Robak T, Jamroziak K, Gora-Tybor J, Stella-Holowiecka B, Konopka L, Ceglarek B et al. Comparison of cladribine plus cyclophosphamide with fludarabine plus cyclophosphamide as first-line therapy for chronic lymphocytic leukemia: a phase III randomized study by the Polish Adult Leukemia Group (PALG-CLL3 Study). *J Clin Oncol* 2010; **28**: 1863–1869.

5 Hallek M, Fischer K, Fingerle-Rowson G, Fink AM, Busch R, Mayer J et al. Addition of rituximab to fludarabine and cyclophosphamide in patients with chronic lymphocytic leukaemia: a randomised, open-label, phase 3 trial. *Lancet* 2010; **376**: 1164–1174.

6 Christian BA, Lin TS. Antibody therapy for chronic lymphocytic leukemia. *Semin Hematol* 2008; **45**: 95–103.

7 Cartron G, Watier H, Golay J, Solal-Celigny P. From the bench to the bedside: ways to improve rituximab efficacy. *Blood* 2004; **104**: 2635–2642.

8 de Haij S, Jansen JH, Boross P, Beurskens FJ, Bakema JE, Bos DL et al. In vivo cytotoxicity of type I CD20 antibodies critically depends on Fc receptor ITAM signaling. *Cancer Res* 2010; **70**: 3209–3217.

9 Mishima Y, Sugimura N, Matsumoto-Mishima Y, Terui Y, Takeuchi K, Asai S et al. An imaging-based rapid evaluation method for complement-dependent cyto-toxicity discriminated clinical response to rituximab-containing chemotherapy. *Clin Cancer Res* 2009; **15**: 3624–3632.

10 Boross P, Jansen JH, de Haij S, Beurskens FJ, van der Poel CE, Bevaart L et al. The in vivo mechanism of action of CD20 monoclonal antibodies depends on local tumor burden. *Haematologica* 2011; **96**: 1822–1830.

11 Di Gaetano N, Cittera E, Nota R, Vecchi A, Grieco V, Scanziani E et al. Complement activation determines the therapeutic activity of rituximab in vivo. *J Immunol* 2003; **171**: 1581–1587.

12 Bannerji R, Kitada S, Flinn IW, Pearson M, Young D, Reed JC et al. Apoptotic-regulatory and complement-protecting protein expression in chronic lymphocytic leukemia: relationship to in vivo rituximab resistance. *J Clin Oncol* 2003; **21**: 1466–1471.

13 Stoiber H, Clivio A, Dierich MP. Role of complement in HIV infection. *Annu Rev Immunol* 1997; **15**: 649–674.

14 Durrant LG, Spendlove I. Immunization against tumor cell surface complement-regulatory proteins. *Curr Opin Invest Drugs* 2001; **2**: 959–966.

15 Hu W, Ge X, You T, Xu T, Zhang J, Wu G et al. Human CD59 inhibitor sensitizes rituximab-resistant lymphoma cells to complement-mediated cytolysis. *Cancer Res* 2011; **71**: 2298–2307.

16 Markiewski MM, Lambris JD. Is complement good or bad for cancer patients? A new perspective on an old dilemma. *Trends Immunol* 2009; **30**: 286–292.

17 Weng WK, Levy R. Expression of complement inhibitors CD46, CD55, and CD59 on tumor cells does not predict clinical outcome after rituximab treatment in follicular non-Hodgkin lymphoma. *Blood* 2001; **98**: 1352–1357.

18 Golay J, Lazzari M, Facchinetti V, Bernasconi S, Borleri G, Barbui T et al. CD20 levels determine the in vitro susceptibility to rituximab and complement of B-cell chronic lymphocytic leukemia: further regulation by CD55 and CD59. *Blood* 2001; **98**: 3383–3389.

19 Gorter A, Meri S. Immune evasion of tumor cells using membrane-bound complement regulatory proteins. *Immunol Today* 1999; **20**: 576–582.

20 Haeney MR. The role of the complement cascade in sepsis. *J Antimicrob Chemother* 1998; **41**(Suppl A): 41–46.

21 Rodríguez de Córdoba S, Esparza-Gordillo J, Goicoechea de Jorge E, Lopez-Trascasa M, Sánchez-Corral P. The human complement factor H: functional roles, genetic variations and disease associations. *Mol Immunol* 2004; **41**: 355–367.

22 Junnikkala S, Jokiranta TS, Friese MA, Jarva H, Zipfel PF, Meri S. Exceptional resistance of human H2 glioblastoma cells to complement-mediated killing by expression and utilization of factor H and factor H-like protein 1. *J Immunol* 2000; **164**: 6075–6081.

23 Gasque P, Julen N, Ischenko AM, Picot C, Mauger C, Chauzy C et al. Expression of complement components of the alternative pathway by glioma cell lines. *J Immunol* 1992; **149**: 1381–1387.

24 Junnikkala S, Hakulinen J, Jarva H, Manuelian T, Bjørge L, Bützow R et al. Secretion of soluble complement inhibitors factor H and factor H-like protein (FHL-1) by ovarian tumour cells. *Br J Cancer* 2002; **87**: 1119–1127.

25 Fedarko NS, Fohr B, Robey PG, Young MF, Fisher LW. Factor H binding to bone sialoprotein and osteopontin enables tumor cell evasion of complement-mediated attack. *J Biol Chem* 2000; **275**: 16666–16672.

26 Ajona D, Hsu YF, Corrales L, Montuenga LM, Pio R. Down-regulation of human complement factor H sensitizes non-small cell lung cancer cells to complement attack and reduces in vivo tumor growth. *J Immunol* 2007; **178**: 5991–5998.

27 Saunders RE, Goodship TH, Zipfel PF, Perkins SJ. An interactive web database of factor H-associated hemolytic uremic syndrome mutations: insights into the structural consequences of disease-associated mutations. *Hum Mutat* 2006; **27**: 21–30.

28 Schmidt CQ, Herbert AP, Hocking HG, Uhrín D, Barlow PN. Translational mini-review series on complement factor H: structural and functional correlations for factor H. *Clin Exp Immunol* 2008; **151**: 14–24.

29 Schmidt CQ, Herbert AP, Kavanagh D, Gandy C, Fenton CJ, Blaum BS et al. A new map of glycosaminoglycan and C3b binding sites on factor H. *J Immunol* 2008; **181**: 2610–2619.

30 Oppermann M, Manuelian T, Józsi M, Brandt E, Jokiranta TS, Heinen S et al. The C-terminus of complement regulator Factor H mediates target recognition: evidence for a compact conformation of the native protein. *Clin Exp Immunol* 2006; **144**: 342–352.

31 Ferreira VP, Herbert AP, Hocking HG, Barlow PN, Pangburn MK. Critical role of the C-terminal domains of factor H in regulating complement activation at cell surfaces. *J Immunol* 2006; **177**: 6308–6316.

32 Herbert AP, Uhrín D, Lyon M, Pangburn MK, Barlow PN. Disease-associated sequence variations congregate in a polyanion recognition patch on human factor H revealed in three-dimensional structure. *J Biol Chem* 2006; **281**: 16512–16520.

33 Blackmore TK, Hellwage J, Sadlon TA, Higgs N, Zipfel PF, Ward HM et al. Identification of the second heparin-binding domain in human complement factor H. *J Immunol* 1998; **160**: 3342–3348.

34 Perkins SJ, Nan R, Okemefuna AI, Li K, Khan S, Miller A. Multiple interactions of complement Factor H with its ligands in solution: a progress report. *Adv Exp Med Biol* 2010; **703**: 25–47.

35 Bellosillo B, Villamor N, López-Guillermo A, Marcé S, Esteve J, Campo E et al. Complement-mediated cell death induced by rituximab in B-cell lymphoproli-ferative disorders is mediated in vitro by a caspase-independent mechanism involving the generation of reactive oxygen species. *Blood* 2001; **98**: 2771–2777.

36 van Meerten T, van Rijn RS, Hol S, Hagenbeek A, Ebeling SB. Complement-induced cell death by rituximab depends on CD20 expression level and acts complementary to antibody-dependent cellular cytotoxicity. *Clin Cancer Res* 2006; **12**: 4027–4035.

37 Golay J, Zaffaroni L, Vaccari T, Lazzari M, Borleri GM, Bernasconi S et al. Biologic response of B lymphoma cells to anti-CD20 monoclonal antibody rituximab in vitro: CD55 and CD59 regulate complement-mediated cell lysis. *Blood* 2000; **95**: 3900–3908.

38 Harjunpää A, Junnikkala S, Meri S. Rituximab (anti-CD20) therapy of B-cell lymphomas: direct complement killing is superior to cellular effector mechanisms. *Scand J Immunol* 2000; **51**: 634–641.

39 Wilk E, Witte T, Marquardt N, Horvath T, Kalippke K, Scholz K et al. Depletion of functionally active CD20+ T cells by rituximab treatment. *Arthritis Rheum* 2009; **60**: 3563–3571.

40 Golay J, Cittera E, Di Gaetano N, Manganini M, Mosca M, Nebuloni M et al. The role of complement in the therapeutic activity of rituximab in a murine B lymphoma model homing in lymph nodes. *Haematologica* 2006; **91**: 176–183.

41 Beers SA, Chan CH, French RR, Cragg MS, Glennie MJ. CD20 as a target for therapeutic type I and II monoclonal antibodies. *Semin Hematol Apr* **47**: 107–114.

42 Zent CS, Secreto CR, LaPlant BR, Bone ND, Call TG, Shanafelt TD et al. Direct and complement dependent cytotoxicity in CLL cells from patients with high-risk early-intermediate stage chronic lymphocytic leukemia (CLL) treated with alemtuzumab and rituximab. *Leuk Res* 2008; **32**: 1849–1856.

43 Klepfish A, Rachmilewitz EA, Kotsianidis I, Patchenko P, Schattner A. Adding fresh frozen plasma to rituximab for the treatment of patients with refractory advanced CLL. *QJM* 2008; **101**: 737–740.

44 Xu W, Miao KR, Zhu DX, Fang C, Zhu HY, Dong HJ et al. Enhancing the action of rituximab by adding fresh frozen plasma for the treatment of fludarabine refractory chronic lymphocytic leukemia. *Int J Cancer* 2011; **128**: 2192–2201.

45 Giddings KS, Zhao J, Sims PJ, Tweten RK. Human CD59 is a receptor for the cholesterol-dependent cytolysin intermedilysin. *Nat Struct Mol Biol* 2004; **11**: 1173–1178.

46 Charbonneau B, Maurer MJ, Fredericksen ZS, Zent CS, Link BK, Novak AJ *et al.* Germline variation in complement genes and event-free survival in follicular and diffuse large B-cell lymphoma. *Am J Hematol* 2012; **87**: 880–885.

47 Davila S, Wright VJ, Khor CC, Sim KS, Binder A, Breunis WB *et al.* Genome-wide association study identifies variants in the CFH region associated with host susceptibility to meningococcal disease. *Nat Genet* 2010; **42**: 772–776.

48 Jak M, van Bochove GG, van Lier RA, Eldering E, van Oers MH.. CD40 stimulation sensitizes CLL cells to rituximab-induced cell death. *Leukemia* 2011; **25**: 968–978.

49 Loffler A, Gruen M, Wuchter C, Schriever F, Kufer P, Dreier T *et al.* Efficient elimination of chronic lymphocytic leukaemia B cells by autologous T cells with a bispecific anti-CD19/anti-CD3 single-chain antibody construct. *Leukemia* 2003; **17**: 900–909.

Supplementary Information accompanies this paper on the Leukemia website (http://www.nature.com/leu)